32nd Electric Vehicle Symposium (EVS32)
Lyon, France, May 19 - 22, 2019

Scalable and Accurate Modelling of a WBG-based Bidirectional DC/DC Converter for Electric Drivetrains

Sajib Chakraborty[1,2], Yuanfeng Lan[1,2], Iosu Aizpuru[3], Mikel Mazuela[3], Argiñe Alacano[3] and Omar Hegazy[1,2*]

[1]*Vrije Universiteit Brussel (VUB), ETEC Department & MOBI Research Group, Pleinlaan 2,1050 Brussels, Belgium;*
[2]*Flanders Make, 3001 Heverlee, Belgium*
[3]*Mondragon Unibertsitatea, Electronics and computing Department, Loramendi, 4;20500 Arrasate-Mondragón (Spain)*
**Correspondence: omar.hegazy@vub.be*

Summary

This article presents the scalable and accurate modelling technique of a Wideband Gap-based (WBG) bidirectional DC/DC converter to achieve high efficiency while satisfying a set of design constraints. Using Si and SiC-based switches, the converter is scaled for different power ratings (10kW~50kW). Moreover, to scale the passive components of the DC/DC converter empirical design approach is developed for inductor while the systematic approach is used for capacitor selection. The accuracy (~95% accurate) of the inductor design approach is verified by the Finite Element Method (FEM) COMSOL software and accurate loss model is validated using the MATLAB tool Simulink®. The proposed study reduces 60% of core losses in comparing with a conventional silicon core, reduces 2.5% of output voltage ripples while maximum efficiency is obtained up to 98.5% at 30kW load using CAS120M12BM2 SiC MOSFET module.

Keywords: Scalability, DC/DC converter, WBG-semiconductors, efficiency, Electric drivetrains.

1 Introduction

Bidirectional DC/DC converters have several advantages, with features such as minimal input current ripples and output voltage ripples, compact size, and bidirectional power flow with a straightforward dual loop control technique [1]. In this article, the bidirectional DC/DC converter topology is designed for scalability and accurate modelling, which consists of three active bridges, as shown in Fig 1. In electric drivetrain during traction operation, the bidirectional DC/DC converter works in boost mode and battery provides power to the electric motor. During deceleration operation, the converter works in buck mode and battery recaptures the regenerative-braking power. Currently, the bidirectional converter has become popular for vehicular drivetrains, photovoltaic microgrids, power distribution systems and charger applications [2]–[5].

In this article, the detailed scalable modelling approach of the bidirectional DC/DC converter is demonstrated, which uses different switching technologies (Si and SiC) at different power levels. To upscale the power level of the DC/DC converter, the voltage and current are easily scaled by selecting the proper

switching rate. A detail database has been prepared for semiconductor modules (Si and SiC) and based on the specifications, the proper device needs to be selected for the power circuit of the bidirectional converter.

However, the primary challenge in the DC/DC converter is to scale the passive components such as inductors and capacitor [6]. For the inductors, the empirical approach is used to estimate the relationship between the inductor airgap and number of turns, the inductor value and the inductor current, while a fast design technique is used to evaluate the total inductor weight according to the inductor current ripples. For the capacitor scaling, the equivalent series resistance (ESR) is used to scale the DC link capacitor. The capacitor design is based on the effect of ESR over frequency range and temperature (^{0}C).

This article also presents accurate modelling approach for the bidirectional DC/DC converter. The accuracy is compared with the Finite Element Method (FEM). Finally, the converter losses are estimated as a function of voltage, current and energy losses from the switch datasheet based on analytic approaches with high accuracy and for calculating inductor losses and conduction losses, core geometry and ESR are taken into consideration.

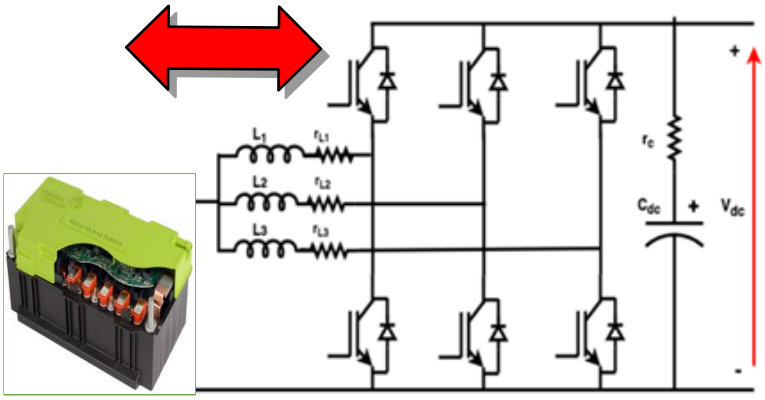

Figure 1. Bi-directional DC/DC converter model.

2 Device Modelling

2.1 MOSFET structure and modelling techniques

The Metal Oxide Semiconductor Field Effect Transistor (MOSFET) is composed of a MOS field, which gives the idea about its construction and a FET field, which speaks about its working principle. The MOSFET gained importance with respect to the bipolar junction transistor thanks to its unipolar behavior and the voltage-controlled gate characteristics. There are three classical semiconductor modelling techniques that can be used to model the MOSFET's static and dynamic behaviors as shown in Figure 2.

Physical models are represented by the composition of the internal silicon-based layers of the semiconductors. They are very accurate, but we need precise information about the internal structure of the device. Manufacturers usually do not give this information. Furthermore, they are time-consuming, so they are not used for big time simulations [7].

The electrical equivalent model is used to analyze the conduction and switching behavior of the semiconductors. The models are accurate but highly nonlinear due to voltage dependency of equivalent capacitances presented in the semiconductor structure. The simulation speed is low because the switching behavior should be simulated in detail [8].

The universal losses model separates the conduction behavior and the switching behaviour of the semiconductor. It simulates the switching behaviour oriented to power losses in a single simulation step, which permits to increase the simulation speed. This type of models is accurate enough and allow modelling in detail the thermal and electrical behavior of the semiconductors, without compromising simulation speed [9].

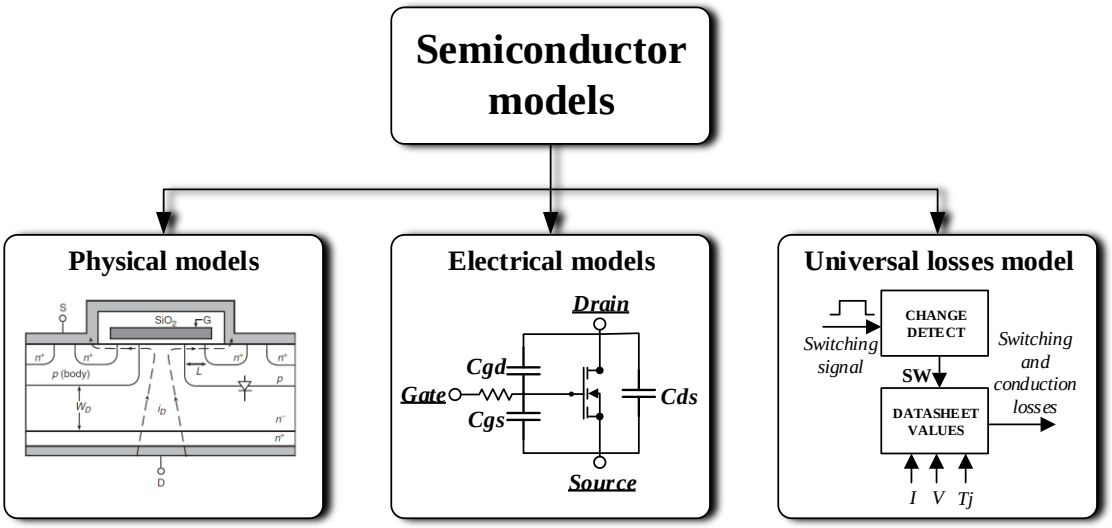

Figure 2. Three main semiconductor/MOSFET models: Physical models [7], Electrical equivalent models [8]and Universal losses models [9].

2.2 Conduction and switching losses modelling

As described in [9], the universal losses model has been proven as a perfect solution to achieve a good tradeoff between the accuracy and computational cost. Thus, the universal losses model has been developed in this work for modelling of the electrical behavior of the semiconductors. The idea consists basically in implementing the semiconductors as ideal switches (Figure 3(a) and (c) for MOSFET and diode respectively) and estimating in parallel its power losses (Figure 3(b) and (d) for MOSFET and diode respectively). For that purpose, the gate signals of the active semiconductors are also considered ideal. Although different power losses can be described during the semiconductor's operation, the conduction and switching losses are mainly responsible for its electro-thermal behavior.

On the one hand, when a MOSFET is turned on, it behaves like a gate (G) controlled ideal switch with an on-resistance $R_{DS,on}$ connected in series, Figure 3(b). Depending on the required model accuracy, this resistive characteristic can be modelled as an ideal conductor (null resistance), a constant resistance (usually in the range of milliohms) or a junction temperature dependent resistance.

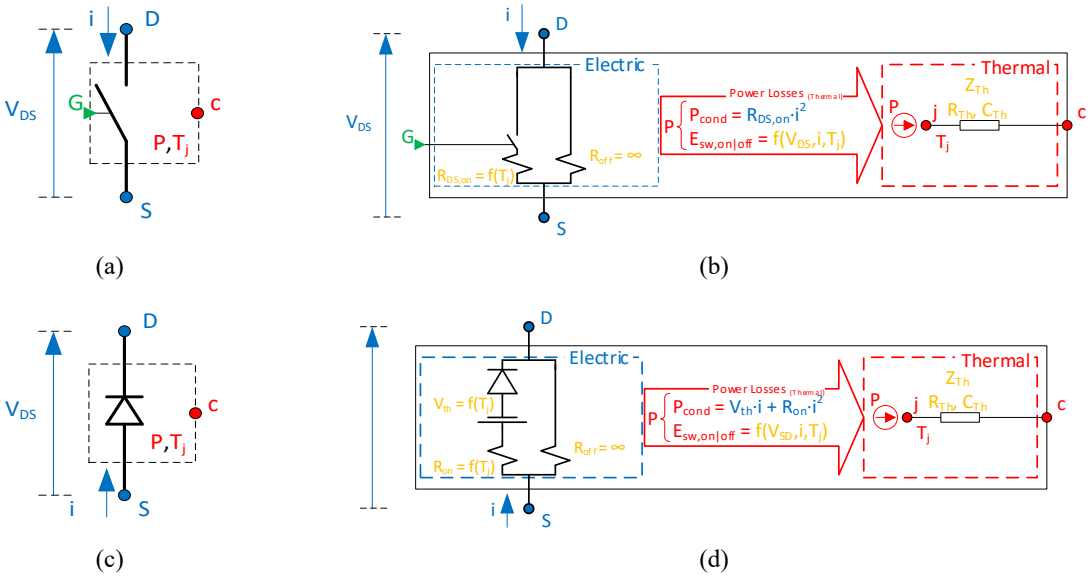

Figure 3. MOSFET electro-thermal model diagram: Switch model (a,b) and Body diode model (c,d).

A similar approach can be made for the antiparallel Body diode that appears in the MOSFET structure. Diodes are usually modelled by means of the series connection of a voltage drop (V_{th}) and an on the resistor (R_{on}) as shown in Figure 3(b) and both of them can be modelled as ideal (null), constant or junction temperature-dependent elements.

On the other hand, the switching losses appear during the turn-on and turn-off transition of the semiconductors, due to their non-ideal voltage and current transitions, which produce an eventual coexistence of voltage and current. In order to avoid high computational cost simulations, the universal losses model considers turn-on and turn-off commutations of the MOSFET as ideal transitions, that is, considering instantaneous commutations and ignoring the transient overvoltage, Figure 4 (a). Power losses produced in each transition are added afterward as instantaneous energy losses ($E_{sw,on}$, $E_{sw,off}$), distributed along a switching step time, Figure 4(b).

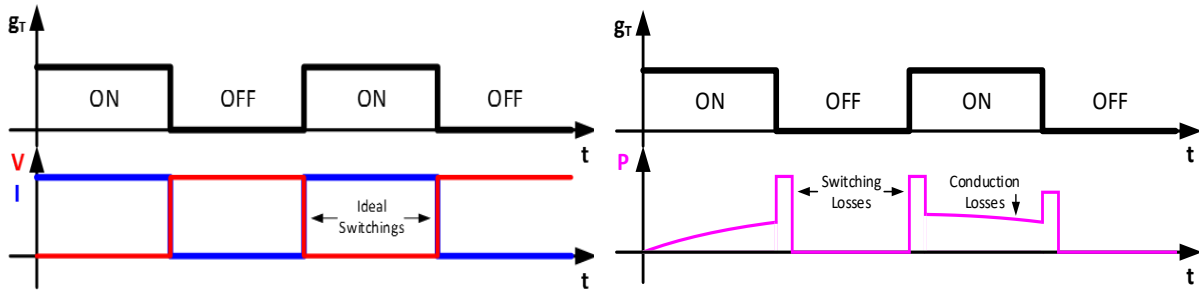

(a) (b)

Figure 4. Electric behavior modelling: (a) Ideal conduction and switching waveforms; (b) Conduction and switching losses estimation.

In order to estimate these switching losses, different degrees of accuracy can be taken into account. On the basis of the switching losses curves given in the datasheet of any semiconductor, $E_{sw,on}$ and $E_{sw,off}$ can be modelled as ideal (null), current dependent (Figure 5(a)), voltage-current dependent (Figure 5(b) or temperature-voltage-current dependent, using different 1, 2 or 3 dimension look-up tables for that purpose.

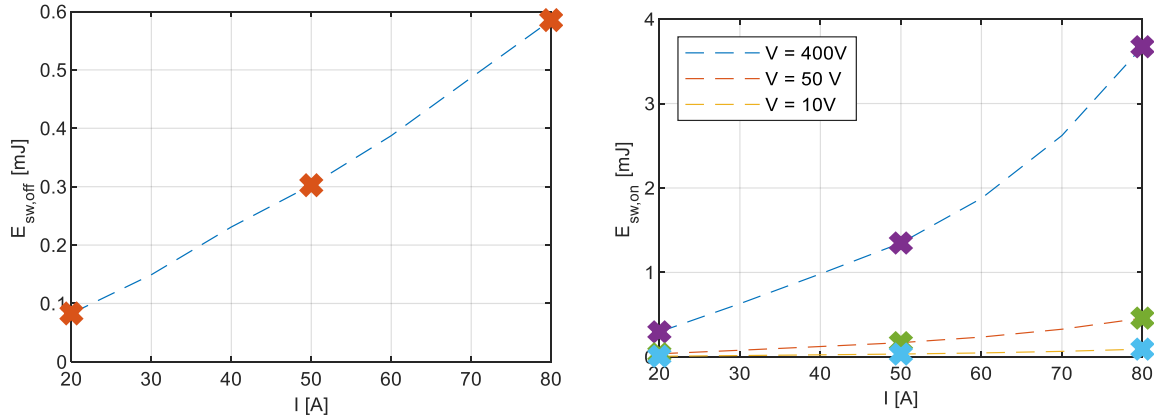

(a) (b)

Figure 5. (a) Current dependent turn-off losses 1D LUT; (b) Voltage and Current dependent turn-on losses 2D LUT.

Both conduction and switching losses are analytically estimated in parallel calculations, taking into account the instantaneous current conducting through the MOSFET or its body diode. These power losses could easily be coupled to the thermal models of the semiconductors and the resulting temperatures could be fed back again to complete the electro-thermal coupling, being able to achieve a high degree of accuracy with a reduced computational cost.

3 Passive Component Modelling

The primary goal is to model high-performance inductors having high relative permeability with low eddy current and high accuracy. These inductors are modelled for achieving high power density and reducing weight while obtaining minimal core losses. The DC link capacitor is selected having low ESR to limit the output voltage ripples and temperature rise.

3.1 Selection of high-performance material

In order to maximize the power density of the inductor, Metglas® Amorphous 2605SA1 is selected as the core material. Figure 6 shows the DC hysteresis loops of conventional M-4 silicon steel and Metglas 2605SA1. Metglas 2605SA1 has remarkably higher permeability than M-4 silicon steel. Each core is a combination of micro-thin ribbons (23µm), which confirms high electrical resistivity and high-power density [10].

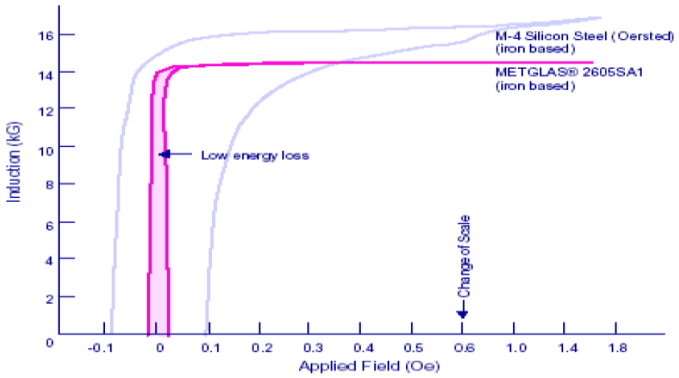

Figure 6. DC hysteresis loops of M-4 silicon steel and Metglas 2605SA1.

3.2 FEM analysis of inductor design

Finite Element Method (FEM) is implemented to simulate the designed inductor. A 2nd-order polynomial fitting function is used to find the inductance value in terms of air-gaps and number of turns as shown in Figure 7 (b). After FEM simulation, optimal air-gap and number of turns of the coil are confirmed. Core loss and air-gap loss in the inductor are also calculated before the implementation of the inductor prototype to ensure minimal core losses. Figure 7(a) shows the FEM result of the flux density distribution and current distribution in the inductor.

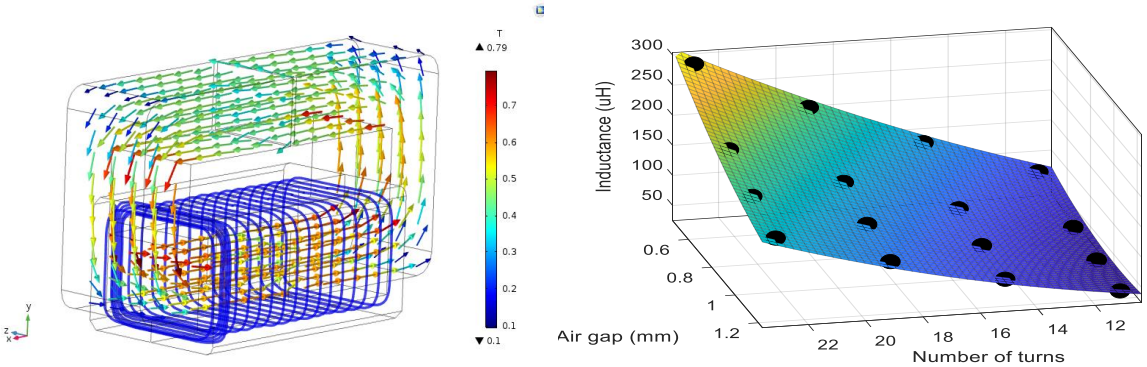

(a) (b)

Figure 7. (a) FEM result of flux density and current distribution, (b) FEM result of inductor design.

3.3 Inductor design and prototype

As the input current ripple and total converter losses are the functions of inductance value, it is necessary to ensure that the real inductance value has a high degree of accuracy with FEM result. Figure 8 (a) depicted the inductor design in SOLIDWORKS, which is used in FEM simulation and (b) prototype of the inductor is shown. The simulation and experimental results are compared in section 5.

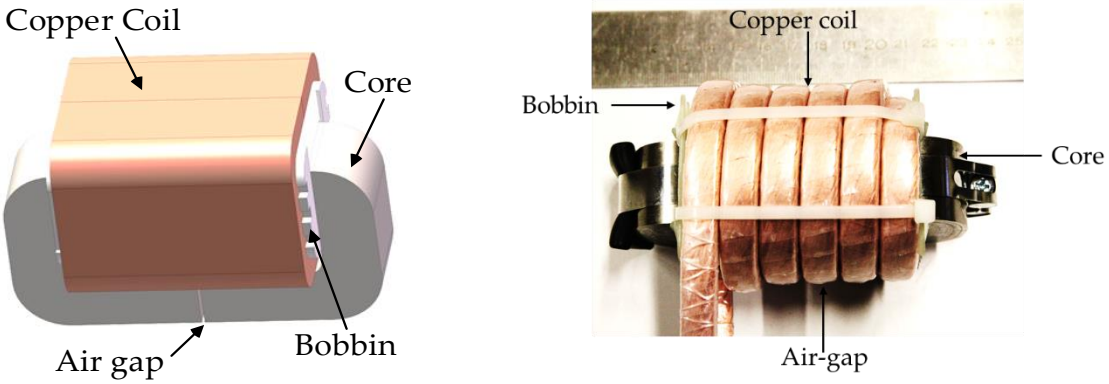

Figure 8. (a) SOLIDWORKS inductor design, (b) a prototype of the inductor.

3.4 Capacitor selection with minimal equivalent series resistance

A function is used for scalable capacitor selection based on Equivalent Series Resistance (ESR) as follows.

$$\mathrm{ESR} = \frac{R_2}{1 + (2\pi f)^2 C_2^2 R_2^2} + R_1 + R_0 \qquad (1)$$

where, R_0=resistance of foil, tabs and terminals (Ω), R_1=resistance of electrolyte (Ω), R_2=dielectric loss resistance (Ω), C_2=dielectric loss capacitance (F), f=frequency (Hz). There are basically two appropriate choices: type 947C and type 947D polypropylene DC link capacitors from Cornell Dubilier for 10kW-50kW power ratings. After comparing both types, type 947C is selected since it offers decidedly smaller ESR, the high capacitance per volume and low voltage ripple and temperature rise. The comparison of ESR as a function of frequency and temperature is shown in Figure 9 which ensures optimum response of type 947C capacitor at the same capacitance level.

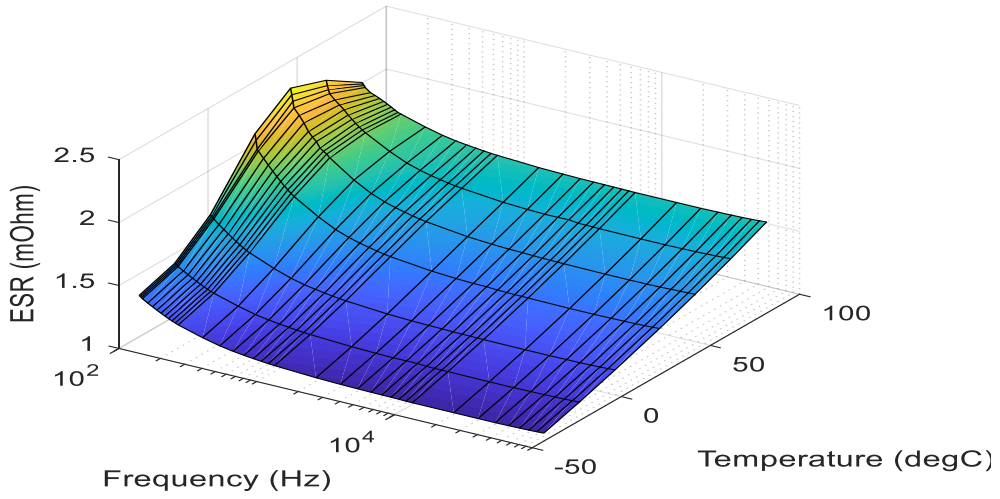

(a)

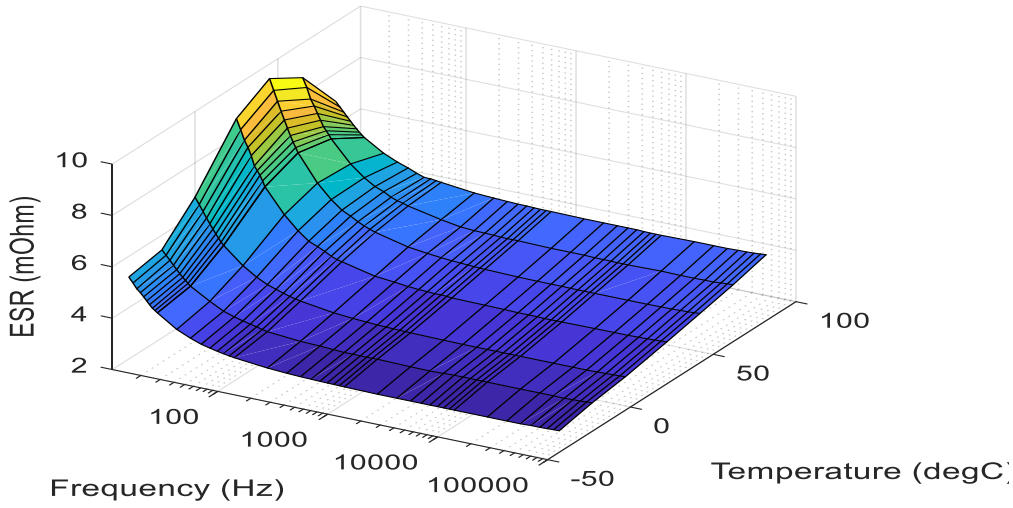

(b)

Figure 9. ESR model of capacitors at same capacitance: (a) Type 947C (b)Type 947D.

4 Accurate Loss Modelling

The losses in interleaved bidirectional DC/DC converter consists of MOSFETs losses (switching losses and conduction losses), inductor losses (core loss, air-gap loss and conduction loss) and ESR losses of the capacitor [11]. During simulation, conduction (power) and switching (energy) losses are analytically estimated using instantaneous current and voltage drop across the MOSFET module (switch and body-diode). Afterward, the instantaneous power losses in the MOSFET module is passed through a median low-pass filter (LPF) having (1/10) switching frequency as the cut-off frequency to obtain DC information contents in the low frequencies, which also speeds up the simulation time while maintaining a high degree of accuracy up to two decimal points. For measuring inductor losses, core geometry is extracting from manufacturer datasheet, and air-gap information is taken from FEM simulation. The expression for calculating inductor losses are derived below. Finally, ESR and internal resistance of inductor Litz wire are used to calculate passive components conduction losses in the DC/DC converter.

$$P_{loss\_inductor} = P_{Core} + P_{CondL} + P_{air-gap} \tag{2}$$

with

$$P_{condL} = I_{L,rms}^2 R_L \tag{3}$$

$$P_{condC} = I_{c,rms}^2 ESR \tag{4}$$

$$P_{core} = W_t(6.5\, f_{sw}^{1.51} B_{ac}^{1.74}) \tag{5}$$

$$P_{air-gap} = k_g L_{g,cm} c^{1.65} f_{sw}^{1.72} B_{ac}^2 \tag{6}$$

and

$$B_{ac} = \frac{0.4\pi N_t \Delta I 10^{-4}}{L_{g,cm}} \tag{7}$$

5 Results and Discussion

Table 1 shows the inductance of the designed prototype and the FEM simulation result. It indicates that there is an exact (~95%) simulated result obtained from FEM simulation.

Table 1: FEM and Experimental result

AMCC50	FEM (μH)	Experimental (μH) Prototype
Number of turns=19; Airgap=0.8mm	155.49	164.8

Figure 10 illustrates the voltage ripple comparison of the bidirectional DC/DC converter and it can be seen that type 947C has a better response (2.5%) comparing with its counterpart.

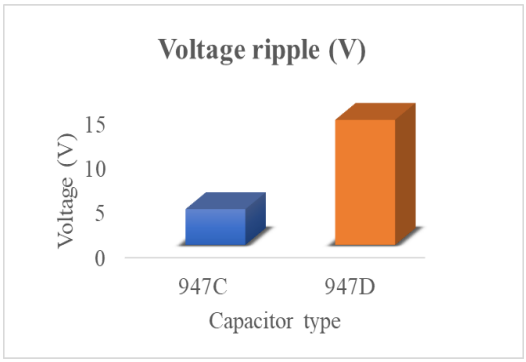

Figure 10. Voltage ripple comparison of the DC/DC converter at fixed output voltage (400V).

Figure 11 shows improved (~60%) core loss response of selected Metglas 2605SA1 core with respect to conventional silicon steel.

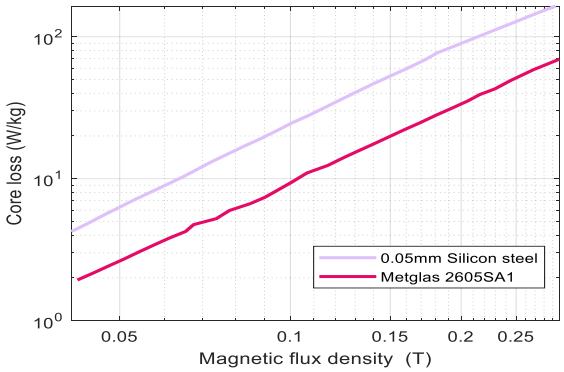

Figure 11. Core loss curve of silicon steel and Metglas 2605SA1 at 20kHz current.

To ensure the superiority of the WBG semiconductor switches over Si the DC/DC converter topology is assessed to measure the converters losses and efficiency. CAS120M12BM2 from Wolfspeed is used as SiC module and SKM400GB12T4 is used as Si module. SiC increases system efficiency significantly in the DC/DC converter compared to Si, by up to 2.7% at 30kW load for 20kHz switching frequency, and by up to 5.1% at 30kW load for 60kHz switching frequency as shown in Figure 13.

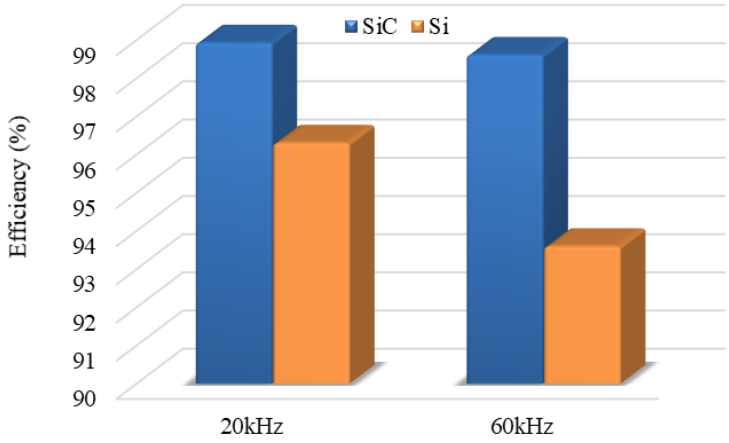

Figure 12. Comparative efficiency measurement of the DC/DC converter at fixed load power.

It can be seen from Figure 13 that the IGBT module (switch and body-diode) losses are higher in case of Si-based converter which reduces comprehensively from SiC-based converter.

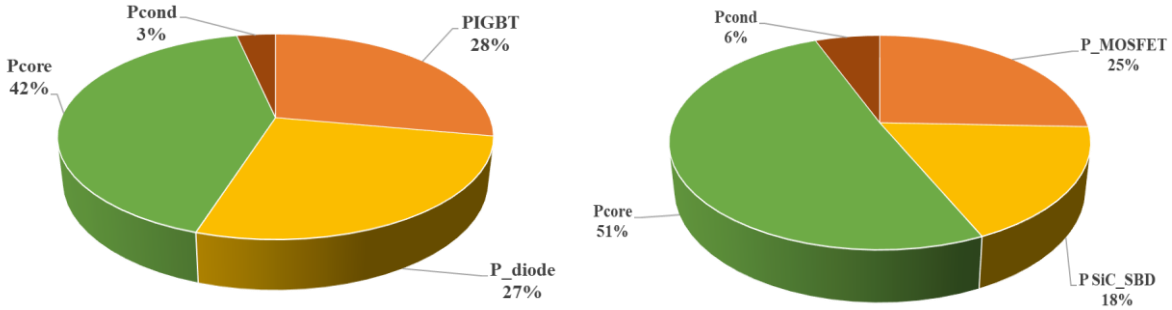

Figure 13. Comparative efficiency measurement of the DC/DC converter at fixed load power.

6 Conclusion

Since the demand for the electric vehicles is increasing at an exponential rate, scalability and highly accurate modelling techniques become a challenging issue for power electronics interfaces. Hence, this paper provides a scalable and accurate modelling technique for bidirectional DC/DC converter in electric drivetrains application. The study shows the impact of the WBG switches on the performance of the DC/DC converter. With the proposed scalable device and passive components, the bidirectional DC/DC converter achieves up to 98.5% efficiency for the entire battery charging profile at 30kW load. Furthermore, the electro-thermal coupling behaviour will be investigated for standard mission profile cycle in the future to observe the impact of temperature on the performance and reliability.

Acknowledgments

This project (HiFi-Elements) has received funding from the European Union's Horizon 2020 research and innovation program under Grant Agreement no. 769935. Authors also acknowledge Flanders make and VLAIO for the support to this research group.

References

[1] E. Nazeraj, O. Hegazy, and J. Van Mierlo, "Control Design , Analysis and Comparative study of Different Control Strategies of a Bidirectional DC / DC Multiport Converter for Electric Vehicles," *Evs30*, pp. 1–14, 2017.

[2] S. Chakraborty, M. M. Hasan, I. Worighi, O. Hegazy, and M. A. Razzak, "Performance Evaluation of a PID-Controlled Synchronous Buck Converter Based Battery Charging Controller for Solar-Powered Lighting System in a Fishing Trawler," *Energies*, vol. 11, no. 10, p. 2722, Oct. 2018.

[3] O. Hegazy, R. Barrero, J. Van Mierlo, P. Lataire, N. Omar, and T. Coosemans, "An Advanced Power Electronics Interface for Electric Vehicles Applications," *IEEE Trans. Power Electron.*, vol. 28, no. 12, pp. 5508–5521, 2013.

[4] M. Forouzesh, Y. P. Siwakoti, S. A. Gorji, F. Blaabjerg, and B. Lehman, "Step-Up DC-DC converters: A comprehensive review of voltage-boosting techniques, topologies, and applications," *IEEE Trans. Power Electron.*, vol. 32, no. 12, pp. 9143–9178, 2017.

[5] L. Pan and C. Zhang, "An integrated multifunctional bidirectional AC/DC and DC/DC converter for electric vehicles applications," *Energies*, vol. 9, no. 7, 2016.

[6] A. Rufer, M. Veenstra, and P. Barrade, *Passive components used in power converters*. EPFL, Lausanne, Switzerland, Tec h.Rep.

[7] M. K. Kazimierczuk, *Pulse-width Modulated DC – DC Power Converters*. 2008.

[8] Y. Cui, M. Chinthavali, and L. M. Tolbert, "Temperature dependent Pspice model of silicon carbide power MOSFET," in *2012 Twenty-Seventh Annual IEEE Applied Power Electronics Conference and Exposition (APEC)*, 2012, pp. 1698–1704.

[9] J. W. Kolar, "A General Scheme for Calculating Switching- and Conduction-Losses of Power Semiconductors in Numerical Circuit Simulations of Power Electronic Systems," in *International Power Electronics Conference (IPEC05), Niigata,Japan, April.*, 2005, pp. 4–8.

[10] Metglas Datasheet: http://elnamagnetics.com/wp-content/uploads/catalogs/Metglas/powerlite.pdf, accessed on 20 Oct. 2018.

[11] D. Tran, S. Chakraborty, Y. Lan, J. Van Mierlo, and O. Hegazy, "Optimized Multiport DC/DC Converter for Vehicle Drivetrains: Topology and Design Optimization," *Appl. Sci.*, 2018.

Authors

	Sajib Chakraborty received his B.Sc. and M.Sc. (with distinction) degrees in Electrical and Electronic Engineering from the Independent University, Bangladesh in 2013 and 2016; respectively. Currently, he is working as a Ph.D. student in the Power Electronics and Electrical Machines (PEEM) team of the MOBI research group at the Vrije Universiteit Brussel. His research interests are including modelling of bidirectional converter, DC/DC power converter for electric drivetrains, scalability and reliability of power electronics converters and renewable energy technology. He is a young professional member of IEEE.
	Yuanfeng Lan received his B.Sc. degree in Engineering from University of Science and Technology Beijing and the M.Sc degree in Engineering from Beijing Jiaotong University, China in 2014 and 2016 respectively. Currently, he is working as a PhD student in the Power Electronics and Electrical Machines (PEEM) team of the MOBI research group at the Vrije Universiteit Brussel. His main research interests include design of Switched Reluctance Machine (SRM), control of SRM, and acoustic analysis of SRM.
	Iosu Aizpuru (PhD'15) received the B.Sc, M.Sc. and PhD in electrical engineering from the University of Mondragon, Spain, in 2006, 2009 and 2015 respectively. He is currently a researcher and lecturer in the Department of Electronics, Faculty of Engineering, Mondragon University. His current research interests include power electronics modelling, energy storage modelling and control of energy storage systems via power electronic converters. He has participated in various research projects in the fields of traction and stationary systems for railway applications, renewable energy applications and energy storage applications for traction, on-grid and off grip systems.
	Mikel Mazuela (PhD'15) received the B.Sc. and M. Sc. Degrees in Electrical Engineering from Mondragon University, Spain, in 2007 and 2010 respectively. He obtained the Ph.D. degree in Electrical Engineering from Mondragon University in 2015. He joined Ingeteam Power Technology in September 2015 where he worked as a R&D Engineer in the Industrial & Marine Drives Business Unit. He joined the Electronics Department of the Mondragon University in 2016 and he currently works as researcher and lecturer. His main research interests include modelling, modulation and control of power converters, multilevel topologies and advanced modulation techniques.

	Argiñe Alacano Loiti (PhD'17) received the B.Sc. degree in Industrial Electronics engineering, the M.Sc. degree in Energy and Power Electronics and the Ph.D. degree in Electric Energy from Mondragon University, Spain, in 2011, 2013 and 2017 respectively. Since 2017, she has been a Lecturer with Mondragon University. Her main research interests include renewable energies, power electronic converters, power transmission and distribution and energy storage systems.
	Prof. Hegazy obtained his PhD degree in July 2012 (with the greatest distinction) from the Dept. of Electrical Machines and Energy Technology (ETEC), Vrije Universiteit Brussel (VUB), Belgium. Prof. Hegazy leads the power electronics and electrical machines (PEEM) team in MOBI Research Center and in ETEC Dept., where he coordinates the research work in this field in several national (i.e. VLAIO (ex. IWT)) projects and European projects (such as SAFEDRIVE, UNPLUGGED, ELIPTIC, ORCA, ASSURED, HiFi Elements, HiPerform, ACHILES, etc.). He is the author of more than 100 scientific publications and two patent applications. Furthermore, he is a member of IEEE, EPE, IEEE Power Electronics Society (PELS), EARPA, EGIA and IEC & BEC standards. Prof. Hegazy fields of interest include power electronics, electrical machines, modelling and optimization techniques, electric and hybrid electric vehicles, Energy management strategies and control systems, battery management systems (BMS), charging infrastructure with V2X strategies, smart local grid and renewable energy.